GSA Data Repository Item 2020024

Mays, C., Vajda, V., Frank, T.D., Fielding, C.R., Nicoll, R.S., Tevyaw, A.P., and McLoughlin, S., 2019, Refined Permian–Triassic floristic timeline reveals early collapse and delayed recovery of south polar terrestrial ecosystems: GSA Bulletin, https://doi.org/10.1130/B35355.1.

Data Repository

Appendix 1. Additional methodological details for palynological counts and ordination analyses.

Table A2. Palynomorph taxa and groups sorted by morphological categories as employed throughout this paper. Note the finer taxonomic divisions for PKHB-1 Count 1. Taxa in bold have been employed herein for regional palynostratigraphic correlation. Morphological categories are based on those of Traverse (2007). "Spp." includes only other species not already listed.

Table A3. Abundance tables of palynomorph groups. All percentages are calculated as a proportion of the respective total palynomorph sample count (N). Average counts for PHKB-1 are calculated from the abundances of both counts 1 and 2. Dashes indicate samples included only in PHKB-1 Count 2. Palynomorph concentration per gram of dried sediment (C) derived by the following calculation (modified from Benninghoff, 1962):

$$C = (N \times L_t) / (L \times M),$$

where N = total palynomorph sample count, L_t = estimated *Lycopodium* spores per spiked sample (= 9666; standard deviation = 671; Maher, 1981), L = *Lycopodium* spores counted, and M = mass of processed dried sediment.

Table A4. Abundance tables of palynofacies groups. All percentages are calculated as a proportion of the respective palynofacies total, either category subtotal (n) or total palynofacies count (N = 500). Palyn = palynomorphs, phyto = phytoclasts, miospores = spores + pollen, - = samples in which *Lycopodium* spore tablets were not included during processing. PHKB-1 palynofacies data are from Fielding et al. (2019).

Table A5. Palynomorph categories for ordination analysis applied to all palynomorph count data. Categories employed in this study are numbered.

Table A6. Stable carbon isotope data for PKHB-1 and CCC-27. PHKB-1 data are from Fielding et al. (2019).

Table A7. List of specimens in Figs 7 and 8, including taxon authorities, sample numbers, slide numbers and England Finder coordinates (Eng. Find. coords); K = kerogen slide.

APPENDIX 1: ADDITIONAL METHODS and REFERENCES CITED

Palynology count methods

Of the 52 palynological samples from PHKB-1, we provide the full palynomorph count data sets of the 44 samples presented by Fielding et al. (2019), including additional data categories that were excluded from that study for brevity; taxa assigned to each taxonomic/ morphological category are outlined in Appendix 2. Twenty-four of these samples were counted a second time by CM ('Count 1'; the remaining specimen counts constitute 'Count 2'; see Appendix 3) for the purpose of verifying the original results of Fielding et al. (2019). The remaining eight samples from PHKB-1 (S014107, S014111, S014112, S014115, S014121, S014122, S014123, S014149), and four samples from CCC-27 (S014165, S014168, S014169, S014171), were barren of palynomorphs, and excluded from the palynomorph counts. All palynomorph counts incorporated ≥250 individual specimens, except for six samples from PHKB-1 (S014097, S014099, S014100, S014105, S014116 and S014141) and three samples from CCC-27 (S014158, S014166, S014167), which failed to meet the prescribed specimen count. Full palynomorph count data are presented in Appendix 3.

Pollen diagrams of PHKB-1 (Figs. 3 and 4) were produced from a composite data set of counts 1 and 2; in samples where both count data were available, an average was calculated and used. Where only Count 2 data were available, these data were employed. Count 2 did not include monolete spores other than *Thymospora* spp. and zonate monolete spores (= *Aratrisporites* spp.). As such, all values of 'other monolete spores' for Count 2 were assigned to zero for the purposes of the pollen diagrams.

Kerogen slides of all 78 samples were produced for palynofacies analysis. Palynofacies data were compiled from counts of 500 individual grains (minimum grain diameter = 5 μm). The following palynofacies categories and subcategories were included in the counts (following the classification of Tyson, 1995): 1, palynomorphs ([a] plant spores, [b] pollen, [c] phytoplankton, [d] fungal remains); 2, phytoclasts ([e] opaque including charcoal, [f] tracheids/rays, [g] other translucent phytoclasts, [h] cuticles/membranous tissues); and 3, amorphous organic matter (AOM; [i] particulate, [j] resin). Full palynofacies count data are presented in Appendix 4.

To estimate productivity (a measure of absolute abundance) per sample, a standardized quantity of an exotic marker spore species was added to the samples during palynological processing (Stockmarr, 1971). For these estimates, selected samples were dried, weighed and one spore tablet of extant *Lycopodium clavatum* per sample was added prior to acidification (for specific samples and lycopodium counts, see appendices 3 and 4). Spore tablets were from Batch 3862, as prepared by the Department of Geology, Lund University (2014); estimated number of spores per tablet = 9,666 ± 6.94% (confidence estimations follow Maher, 1981). These extrinsic *Lycopodium* spores were counted in addition to the total counts for palynofacies and palynomorphs outlined above. By counting these standard markers in parallel with the palynological counts, we employed the relative changes in palynomorphs or palynofacies as a proxy of palynomorph production or total organic production, respectively, for a given time horizon. Specifically, there is an inverse relationship between the *Lycopodium* count and total palynomorphs/palynofacies count; hence, an interval of higher palynomorphs/palynofacies productivity should be reflected by a relatively low *Lycopodium* count. Fluvio-deltaic systems are characterized by variable depositional rates and hydraulic sorting of sediments, including palynomorphs and other organic matter (Brown et al., 2007). Thus, productivity estimates should

only be compared between assemblages from lithofacies of similar grain-size (e.g., claystone, siltstone, or fine sandstone), because these should reflect comparable flow conditions at the site of deposition. In order to control for this variable, siltstone and claystone facies were selected for palynological processing, reflecting minimal depositional transport (Folk, 1980), except where indicated in appendices 3 and 4. Palynomorph concentrations for each sample spiked with *Lycopodium* were calculated by employing the method outlined by Benninghoff (1962; see Appendix 3); however, owing to the low concentrations of counted *Lycopodium* spores, absolute palynomorph concentrations could not be determined reliably for most samples in PHKB-1.

Ordination data treatment and indices

For nMDS, the abundance data needed to be standardized across both well successions, and this was conducted in a series of stages. Firstly, within PHKB-1, Count 1 was selected where possible (because of the higher sample counts), and Count 2 data for the remaining samples in that well. Secondly, data categories shared by both successions could be compared without regrouping, whereas more finely-partitioned data required amalgamation into broader morphological categories ('lumping') which could then be compared across all count data sets. Thirdly, samples were excluded if they failed to meet the minimum palynomorphs count number of 250, including functionally barren samples (14 samples in total from PHKB-1, seven from CCC-27; see Appendix 3). Finally, palynomorph categories that were recorded from single samples ('singletons') were excluded in order to decrease statistical noise.

Ordination analyses were conducted on two versions of the compiled data: 1, relative abundance; and 2, presence/absence. Relative abundances were calculated as a proportion of the total count of each sample, thus standardizing for different count sizes. NMDS ordination analyses were conducted on these relative abundance data, and on two types of transformed fossil data sets: 1, a logarithmic function (e.g., Spicer and Hill, 1979; Slater and Wellman, 2015); and 2, a square root function. These transformations were performed to compress the abundance ranges, without altering their relative rank-orders. The Bray-Curtis similarity index was employed for all variants of the relative abundance data; this is algebraically equivalent to the Bray-Curtis dissimilarity index (Bray and Curtis, 1957). The combination of nMDS and Bray-Curtis index has been demonstrated to be a reliable ordination method for quantitative ecological data (Minchin, 1987). For the presence/absence ordination, all palynomorph group abundances were converted to binary, where the absence of a palynomorph group = 0, and presence = 1. The Jaccard index of similarity was chosen for the presence/absence ordination because it has consistently proven reliable for intergroup differences in binary ecological data (Hubálek, 1982). Ordination analysis was conducted on a binary variant of the data set because, although anomalously high taxon abundances can greatly influence the ordination of abundance data sets, binary data are immune to this effect. A comparison of presence/absence and relative abundance ordinations should reveal which samples are contributing inordinately to the dissimilarity between palynomorph assemblages. Furthermore, both ordination techniques were included in this study because temporal differentiation (biozones) was probably a major factor controlling the differences between assemblages, and these zones are defined partly on taxon acmes and partly on taxon first appearances. Relative abundance ordination is more relevant for differentiating the former, whereas presence/absence ordination should reveal the latter.

REFERENCES CITED

Balme, B.E., and Hennelly, J.P.F., 1956, Trilete sporomorphs from Australian Permian sediments: Australian Journal of Botany, v. 4, p. 240–260, https://doi.org/10.1071/BT9560240.

Balme, B.E., 1970, Palynology of Permian and Triassic strata in the Salt Range and Surghar Range, West Pakistan, *in* Kummel, B., and Teichert, C., eds., Stratigraphic Boundary Problems - Permian and Triassic of West Pakistan: Lawrence, University of Kansas, Special Publications, v. 4, p. 305–453.

Benninghoff, W.S., 1962, Calculation of pollen and spore density in sediments by addition of exotic pollen in known quantities: Pollen et Spores, v. 4, p. 332–333.

Bharadwaj, D.C., and Salujha, S.K., 1964, Sporological study of seam VIII in Raniganj Coalfield, Bihar (India) - Part I. Description of sporae dispersae: Palaeobotanist, v. 12, p. 181–215.

Bray, J.R., and Curtis, J.T., 1957, An ordination of the upland forest communities of Southern Wisconsin: Ecological Monographs, v. 27, p. 325–349, https://doi.org/10.2307/1942268.

Brown, A.G., Carpenter, R.G., and Walling, D.E., 2007, Monitoring fluvial pollen transport, its relationship to catchment vegetation and implications for palaeoenvironmental studies: Review of Palaeobotany and Palynology, v. 147, p. 60–76, https://doi.org/10.1016/j.revpalbo.2007.06.005.

de Jersey, N.J., 1962, Triassic spores and pollen grains from the Ipswich Coalfield: Geological Survey of Queensland Publications, v. 307, p. 1–18.

de Jersey, N.J., and Hamilton, M., 1967, Triassic spores and pollen grains from the Moolayember Formation: Geological Survey of Queensland Publications, v. 336, p. 1–61.

de Jersey, N.J., 1970, Early Triassic miospores from the Rewan Formation: Geological Survey of Queensland Publications, v. 345, p. 1–29.

de Jersey, N.J., 1972, Triassic miospores from the Esk Beds: Geological Survey of Queensland Publications, v. 357, p. 1–40.

de Jersey, N.J., 1979, Palynology of the Permian-Triassic transition in the western Bowen Basin: Geological Survey of Queensland Publications, v. 374, p. 1–39.

de Jersey, N.J., and Raine, J.I., 1990, Triassic and earliest Jurassic miospores from the Murihiku Supergroup, New Zealand: New Zealand Geological Survey Paleontological Bulletin, v. 62, p. 1–164.

Eisenack, A., 1958, *Tasmanites* Newton 1875 und *Leiosphaeridia* n.g. als Gattungen der Hystrichosphaeridea: Palaeontographica Abteilung A, v. 110, p. 1–19.

Elsik, W.C., 1999, *Reduviasporonites* Wilson 1962: synonymy of the fungal organism involved in the Late Permian crisis: Palynology, v. 23, p. 37–41, https://doi.org/10.1080/01916122.1999.9989519.

Fielding, C.R., et al., 2019, Age and pattern of the southern high-latitude continental end-Permian extinction constrained by multiproxy analysis: Nature Communications, v. 10, no. 385, https://doi.org/10.1038/s41467-018-07934-z.

Folk, R.L., 1980, Petrology of Sedimentary Rocks: Austin, Hemphill Publishing Co., 184 p.

Foster, C.B., 1979, Permian plant microfossils of the Blair Athol coal measures, Baralaba coal measures, and basal Rewan Formation of Queensland: Geological Survey of Queensland Publications, v. 372, p. 1–244.

Goubin, N., 1965, Description et répartition des principaux pollenites Permiens, Triasiques et Jurassiques des sondages du Bassin de Morondava (Madagascar): Revue de l'Institut Français du Pétrole, v. 20, p. 1415–1458.
Helby, R., 1970, A Biostratigraphy of the Late Permian and Triassic of the Sydney Basin [Ph.D. thesis]: Sydney, Australia, University of Sydney.
Helby, R., 1973, Review of Late Permian and Triassic palynology of New South Wales: Geological Society of Australia Special Publications, v. 4, p. 141–155.
Hennelly, J.P.F., 1958, Spores and pollens from a Permian-Triassic transition, N.S.W: Proceedings of the Linnean Society of New South Wales, v. 83, p. 363–369.
Hubálek, Z., 1982, Coefficients of association and similarity, based on binary (presence-absence) data: An evaluation: Biological Reviews of the Cambridge Philosophical Society, v. 57, p. 669–689, https://doi.org/10.1111/j.1469-185X.1982.tb00376.x.
Maher, L.J., 1981, Statistics for microfossil concentration measurements employing samples spiked with marker grains: Review of Palaeobotany and Palynology, v. 32, p. 153–191, https://doi.org/10.1016/0034-6667(81)90002-6.
Minchin, P., 1987, An evaluation of the relative robustness of techniques for ecological ordination, *in* Prentice, I.C., and van der Maarel, E., eds., Theory and Models in Vegetation Science: Dordrecht, Springer, Advances in Vegetation Science, v. 8, p. 89–107.
Playford, G., 1965, Plant microfossils from Triassic sediments near Poatina, Tasmania: Journal of the Geological Society of Australia, v. 12, p. 173–210, https://doi.org/10.1080/00167616508728592.
Potonié, R., 1960, Synopsis der Gattungen der Sporae dispersae. III. Teil: Nachträge Sporites, Fortsetzung Pollenites: Mit Generalregister zu Teil I–III, 189 p.
Potonié, R., and Lele, K.M., 1961, Studies in the Talchir Flora of India, 1. Sporae dispersae from the Talchir Beds of South Rewa Gondwana Basin: Palaeobotanist, v. 8, p. 22–37.
Segroves, K.L., 1969, Saccate plant microfossils from the Permian of Western Australia: Grana Palynologica, v. 9, p. 174–227, https://doi.org/10.1080/00173136909436435.
Slater, S.M., and Wellman, C.H., 2015, A quantitative comparison of dispersed spore/pollen and plant megafossil assemblages from a Middle Jurassic plant bed from Yorkshire, UK: Paleobiology, v. 41, p. 640–660, https://doi.org/10.1017/pab.2015.27.
Spicer, R.A., and Hill, C.R., 1979, Principal components and correspondence analyses of quantitative data from a Jurassic plant bed: Review of Palaeobotany and Palynology, v. 28, p. 273–299, https://doi.org/10.1016/0034-6667(79)90029-0.
Stockmarr, J., 1971, Tablets with spores used in absolute pollen analysis: Pollen et Spores, v. 13, p. 615–621.
Tiwari, R.S., 1965, Miospore assemblage in some coals of Barakar Stage (Lower Gondwana) of India: Palaeobotanist, v. 13, p. 168–214.
Tyson, R.V., 1995, Sedimentary Organic Matter: Organic Facies and Palynofacies: London, Chapman & Hall, 615 p, https://doi.org/10.1007/978-94-011-0739-6.
Wilson, L.R., 1962, Permian plant microfossils from the Flowerpot Formation, Greer County: Oklahoma Circulars of the Oklahoma Geology Survey, v. 49, p. 1–50.

Global chronostratigraphy

Palynostratigraphic correlation

Radiometric constraints

248
249
250
251
252
253
254
255
Ma

Triassic
Permian
Early Triassic
Lopingian
Olenekian
Ind.
Changhsingian
Wuch.
Spathian
Smithian
G.
D.

Helby et al. 1987 (E Australia)

Aratrisporites tenuispinosus
P. samoilovichii
L. pellucidus
Protohaploxypinus microcorpus
?

Price 1997 (NE Australia)

APT2
APT1
APP6
APP5

Mantle et al. 2010 (recalibrated to Gradstein et al., 2012)

APT2
APT1
Aratrisporites tenuispinosus
Protohaploxypinus samoilovichii
Lunatisporites pellucidus
P. microcorpus
Playfordiaspora crenulata
Dulhuntyispora parvithola
APP6
APP5

Laurie et al. 2016 (E Australia)

APT2
APT1
Aratrisporites tenuispinosus
Protohaploxypinus samoilovichii
Lunatisporites pellucidus
P. m./P. c.
Dulhuntyispora parvithola
APP6
APP5

Present study + Fielding et al. 2019 (Sydney Basin)

APT2
APT1
Aratrisporites tenuispinosus
Protohaploxypinus samoilovichii
Lunatisporites pellucidus
P. microcorpus
P. crenulata
'Dead zone'
Dulhuntyispora parvithola
APP6
APP5

1
1
2
1
1
1
EPE

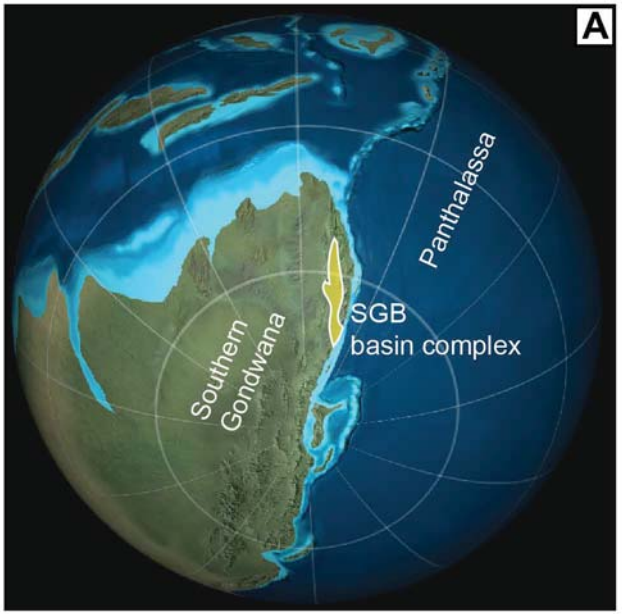
A
Panthalassa
SGB
basin complex
Southern
Gondwana

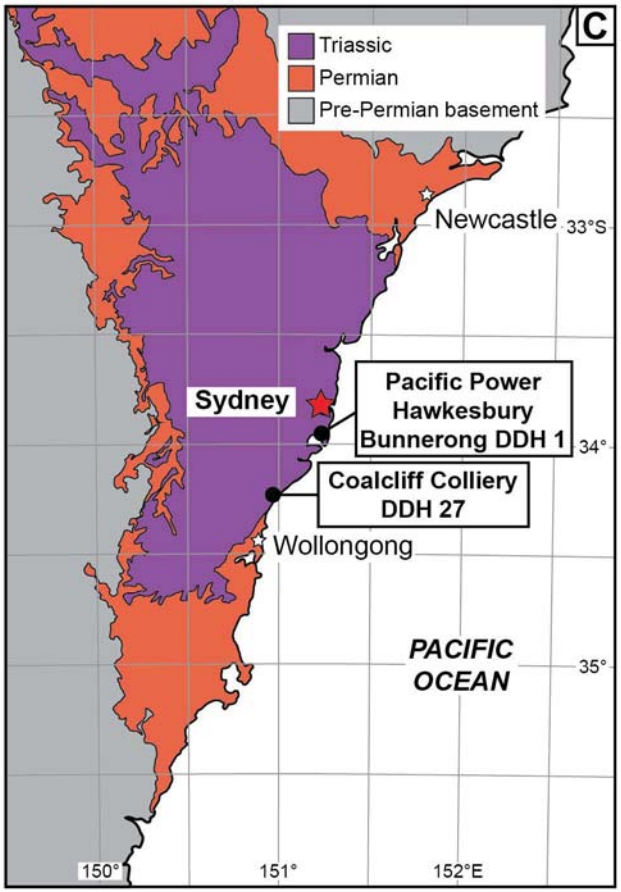
C
Triassic
Permian
Pre-Permian basement
Newcastle
33°S
Sydney
Pacific Power
Hawkesbury
Bunnerong DDH 1
34°
Coalcliff Colliery
DDH 27
Wollongong
PACIFIC
OCEAN
35°
150°
151°
152°E

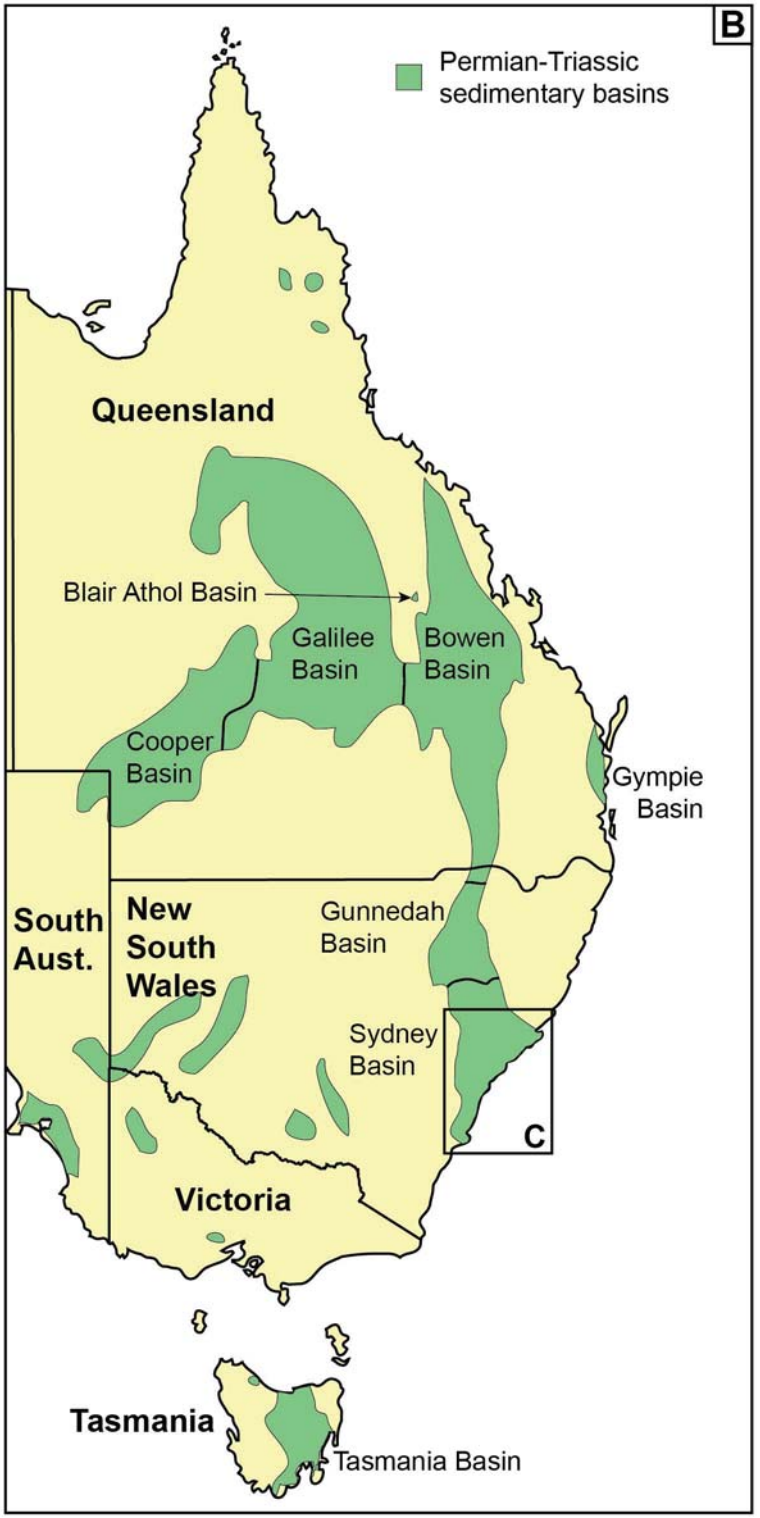
B
Permian-Triassic
sedimentary basins
Queensland
Blair Athol Basin
Galilee
Basin
Bowen
Basin
Cooper
Basin
Gympie
Basin
South
Aust.
New
South
Wales
Gunnedah
Basin
Sydney
Basin
C
Victoria
Tasmania
Tasmania Basin

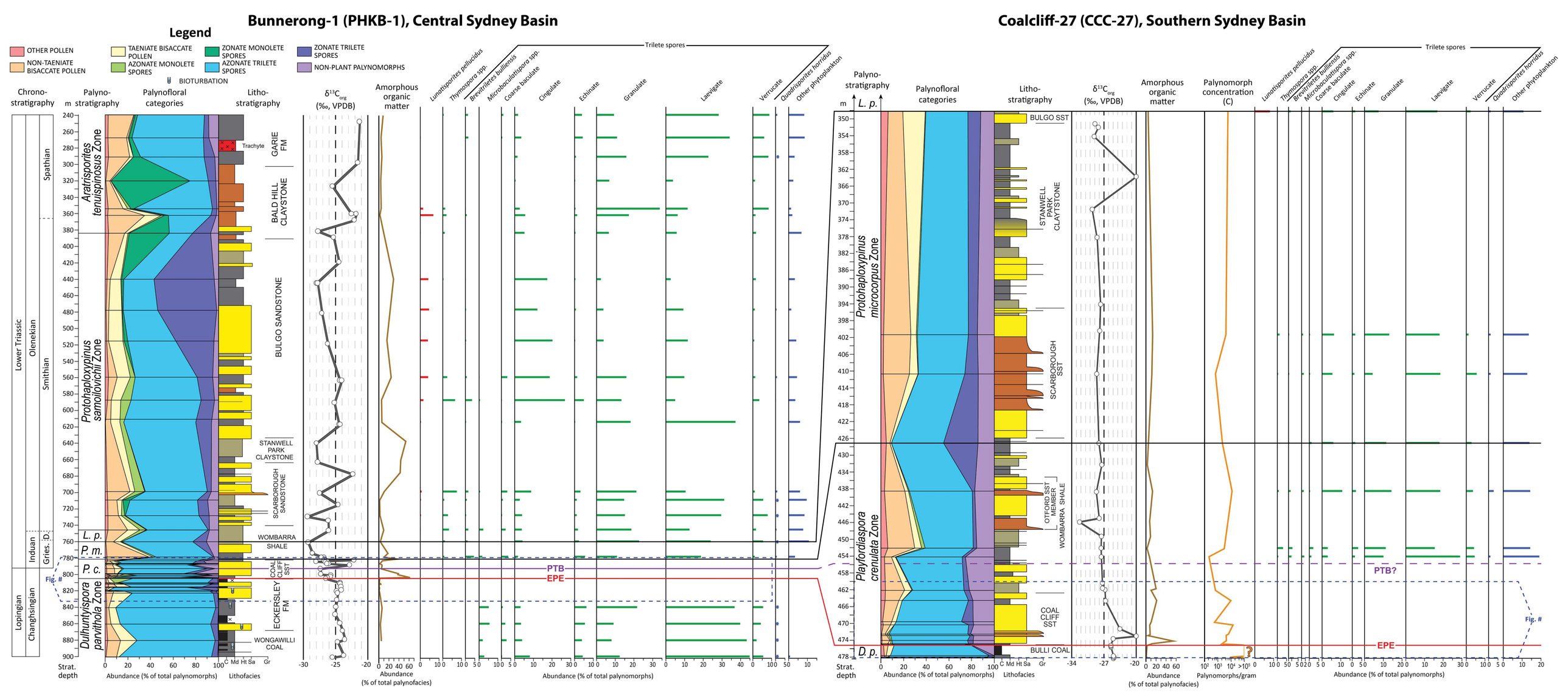
Bunnerong-1 (PHKB-1), Central Sydney Basin
Coalcliff-27 (CCC-27), Southern Sydney Basin
Legend
OTHER POLLEN
NON-TAENIATE BISACCATE POLLEN
TAENIATE BISACCATE POLLEN
AZONATE MONOLETE SPORES
ZONATE MONOLETE SPORES
AZONATE TRILETE SPORES
ZONATE TRILETE SPORES
NON-PLANT PALYNOMORPHS
BIOTURBATION
Chrono-stratigraphy
Palyno-stratigraphy
Palynofloral categories
Litho-stratigraphy
δ13Corg (‰, VPDB)
Amorphous organic matter
Palynomorph concentration (C)
Trilete spores
Lunatisporites pellucidus
Thymospora spp.
Brevitriletes bullienis
Microbaculatisporo spp.
Coarse baculate
Cingulate
Echinate
Granulate
Laevigate
Verrucate
Quadrisporites horridus
Other phytoplankton
Lower Triassic
Lopingian
Changhsingian
Olenekian
Induan
Griesbachian
Smithian
Spathian
Aratrisporites tenuispinosus Zone
Protohaploxypinus samoilovichii Zone
Dulhuntyispora parvithola Zone
Protohaploxypinus microcorpus Zone
Playfordiaspora crenulata Zone
L. p.
P. m.
P. c.
D. p.
Trachyte
GARIE FM
BALD HILL CLAYSTONE
BULGO SANDSTONE
STANWELL PARK CLAYSTONE
SCARBOROUGH SANDSTONE
WOMBARRA SHALE
COAL CLIFF SST
ECKERSLEY FM
WONGAWILLI COAL
BULGO SST
STANWELL PARK CLAYSTONE
SCARBOROUGH SST
OTFORD SST MEMBER
WOMBARRA SHALE
COAL CLIFF SST
BULLI COAL
PTB
EPE
PTB?
Fig. #
Strat. depth
Abundance (% of total palynomorphs)
Lithofacies
C Md Ht Sa Gr
Abundance (% of total palynofacies)
Palynomorphs/gram

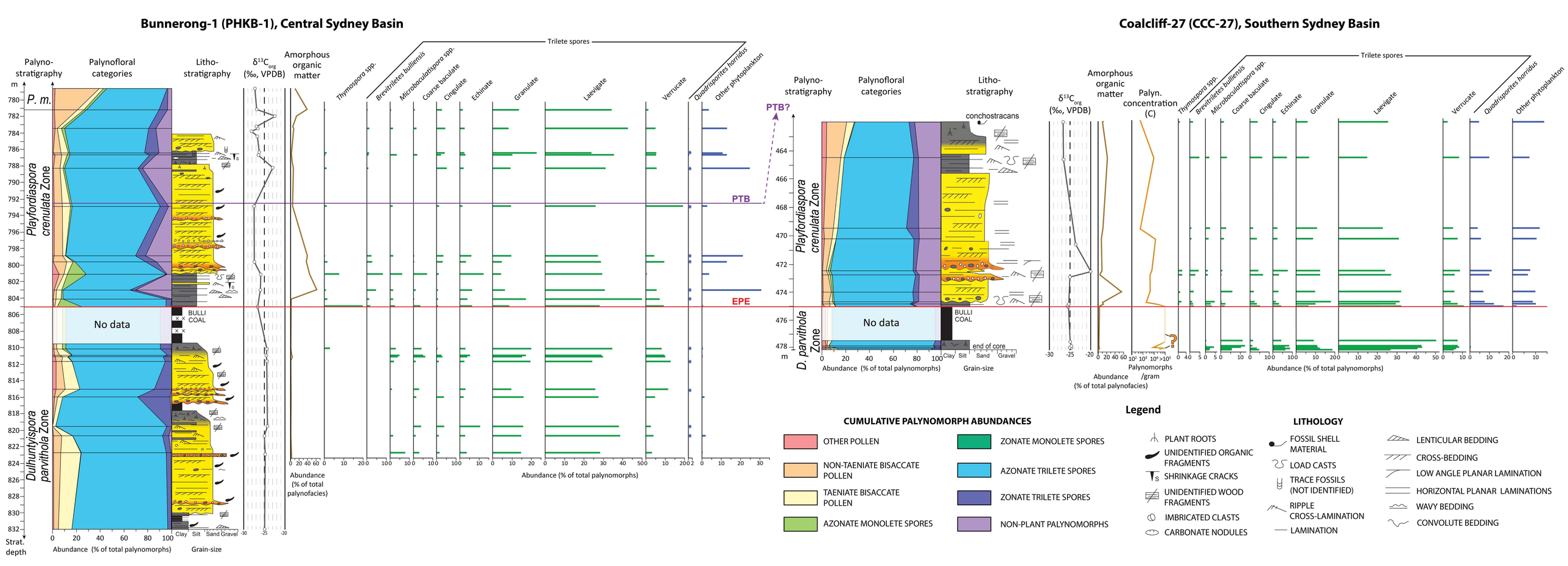
Bunnerong-1 (PHKB-1), Central Sydney Basin
Coalcliff-27 (CCC-27), Southern Sydney Basin
Palyno-stratigraphy
Palynofloral categories
Litho-stratigraphy
δ13Corg (‰, VPDB)
Amorphous organic matter
Trilete spores
Thymospora spp.
Brevitriletes bullensis
Microbaculatispora spp.
Coarse baculate
Cingulate
Echinate
Granulate
Laevigate
Verrucate
Quadrisporites horridus
Other phytoplankton
P. m.
Playfordiaspora crenulata Zone
Dulhuntyispora parvithola Zone
PTB?
PTB
EPE
No data
BULLI COAL
conchostracans
end of core
Strat. depth
m
Abundance (% of total palynomorphs)
Grain-size
Clay
Silt
Sand
Gravel
Abundance (% of total palynofacies)
Palyn. concentration (C)
Palynomorphs /gram
Abundance (% of total palynofacies)
Legend
CUMULATIVE PALYNOMORPH ABUNDANCES
OTHER POLLEN
NON-TAENIATE BISACCATE POLLEN
TAENIATE BISACCATE POLLEN
AZONATE MONOLETE SPORES
ZONATE MONOLETE SPORES
AZONATE TRILETE SPORES
ZONATE TRILETE SPORES
NON-PLANT PALYNOMORPHS
LITHOLOGY
PLANT ROOTS
UNIDENTIFIED ORGANIC FRAGMENTS
SHRINKAGE CRACKS
UNIDENTIFIED WOOD FRAGMENTS
IMBRICATED CLASTS
CARBONATE NODULES
FOSSIL SHELL MATERIAL
LOAD CASTS
TRACE FOSSILS (NOT IDENTIFIED)
RIPPLE CROSS-LAMINATION
LAMINATION
LENTICULAR BEDDING
CROSS-BEDDING
LOW ANGLE PLANAR LAMINATION
HORIZONTAL PLANAR LAMINATIONS
WAVY BEDDING
CONVOLUTE BEDDING

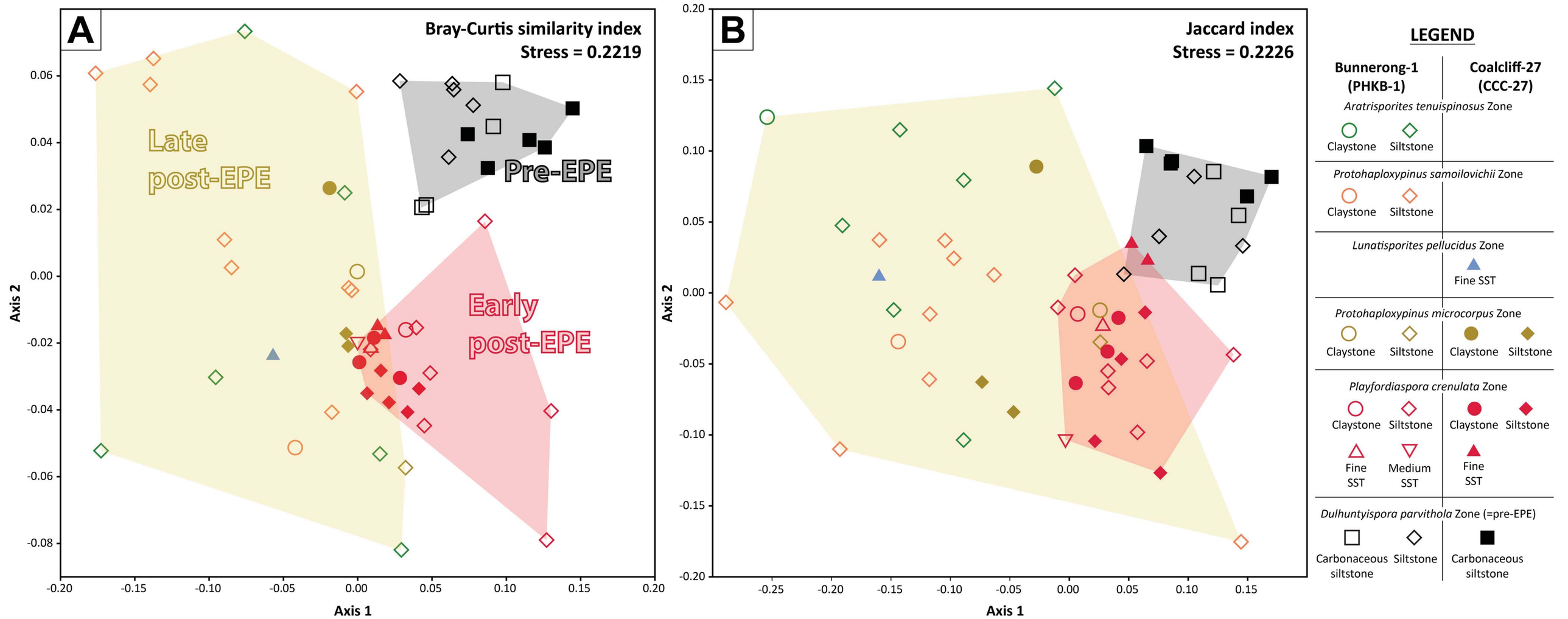
A
Bray-Curtis similarity index
Stress = 0.2219
Late
post-EPE
Pre-EPE
Early
post-EPE
Axis 2
Axis 1
0.06
0.04
0.02
0.00
-0.02
-0.04
-0.06
-0.08
-0.20
-0.15
-0.10
-0.05
0.00
0.05
0.10
0.15
0.20
B
Jaccard index
Stress = 0.2226
Axis 2
Axis 1
0.20
0.15
0.10
0.05
0.00
-0.05
-0.10
-0.15
-0.20
-0.25
-0.20
-0.15
-0.10
-0.05
0.00
0.05
0.10
0.15
LEGEND
Bunnerong-1 (PHKB-1)
Coalcliff-27 (CCC-27)
Aratrisporites tenuispinosus Zone
Claystone
Siltstone
Protohaploxypinus samoilovichii Zone
Claystone
Siltstone
Lunatisporites pellucidus Zone
Fine SST
Protohaploxypinus microcorpus Zone
Claystone
Siltstone
Claystone
Siltstone
Playfordiaspora crenulata Zone
Claystone
Siltstone
Claystone
Siltstone
Fine SST
Medium SST
Fine SST
Dulhuntyispora parvithola Zone (=pre-EPE)
Carbonaceous siltstone
Siltstone
Carbonaceous siltstone

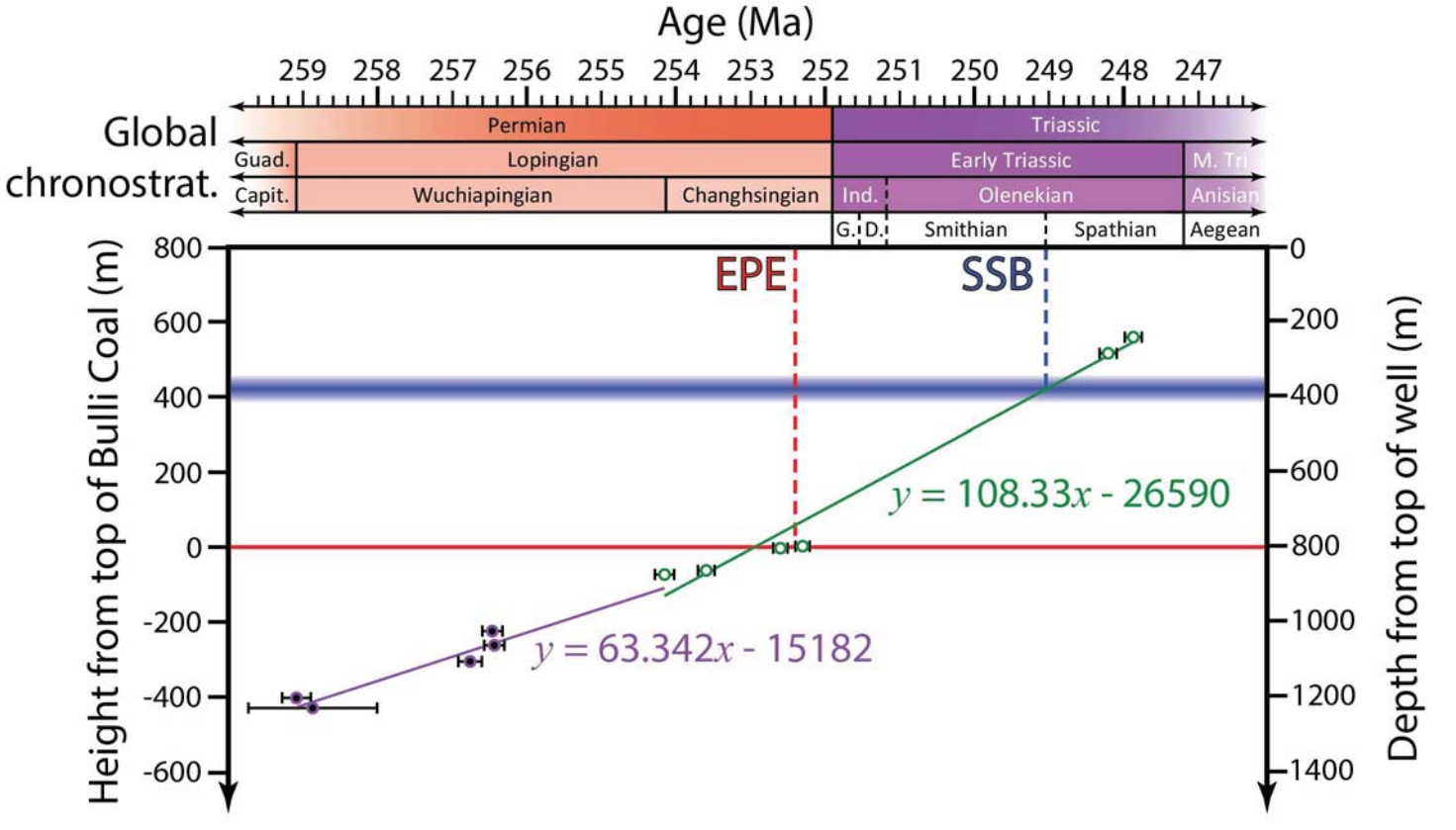
Age (Ma)
259 258 257 256 255 254 253 252 251 250 249 248 247
Global chronostrat.
Permian
Triassic
Guad.
Lopingian
Early Triassic
M. Tri.
Capit.
Wuchiapingian
Changhsingian
Ind.
Olenekian
Anisian
G.
D.
Smithian
Spathian
Aegean
EPE
SSB
y = 108.33x - 26590
y = 63.342x - 15182
Height from top of Bulli Coal (m)
800 600 400 200 0 -200 -400 -600
Depth from top of well (m)
0 200 400 600 800 1000 1200 1400

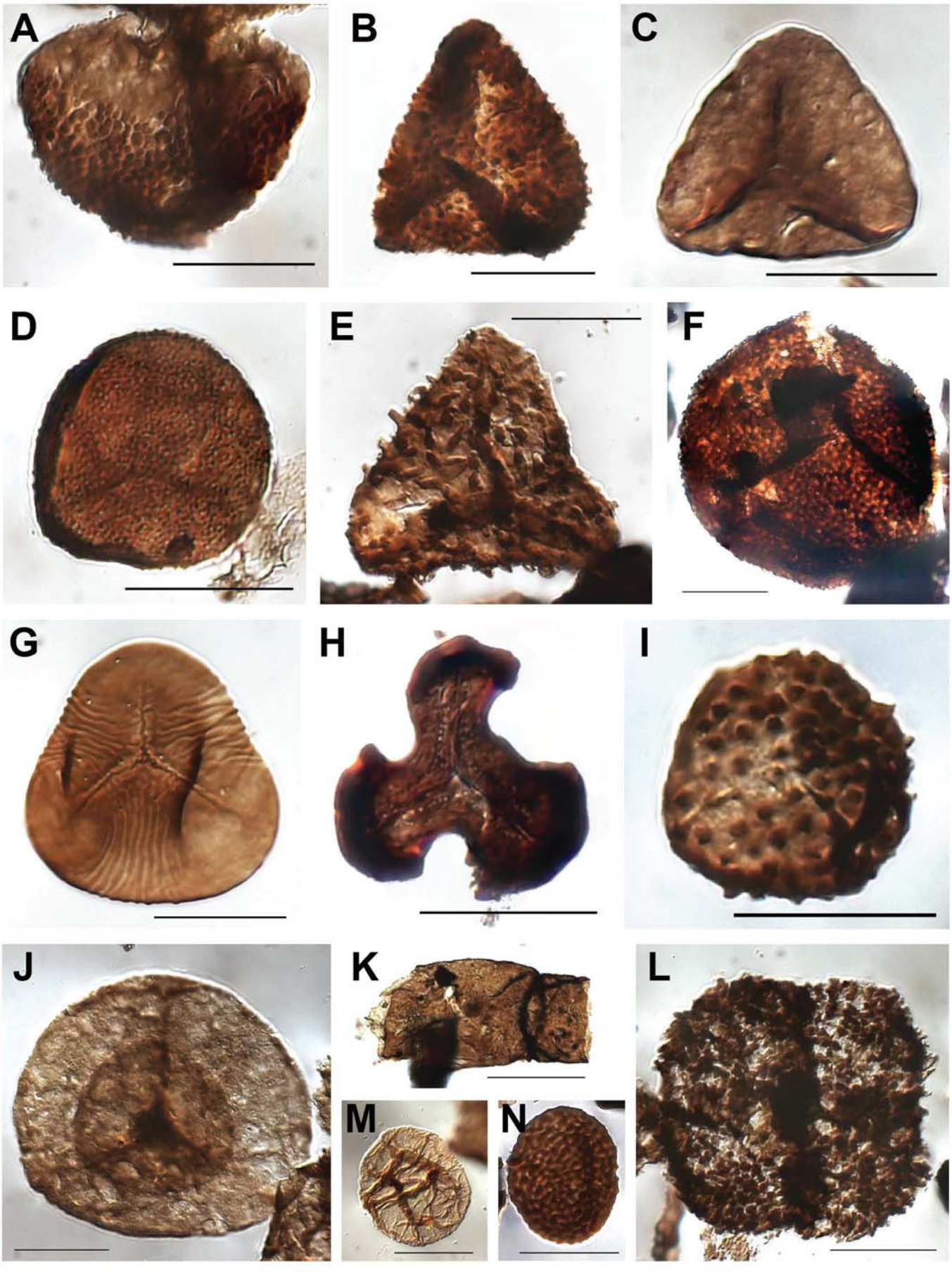
A
B
C
D
E
F
G
H
I
J
K
L
M
N

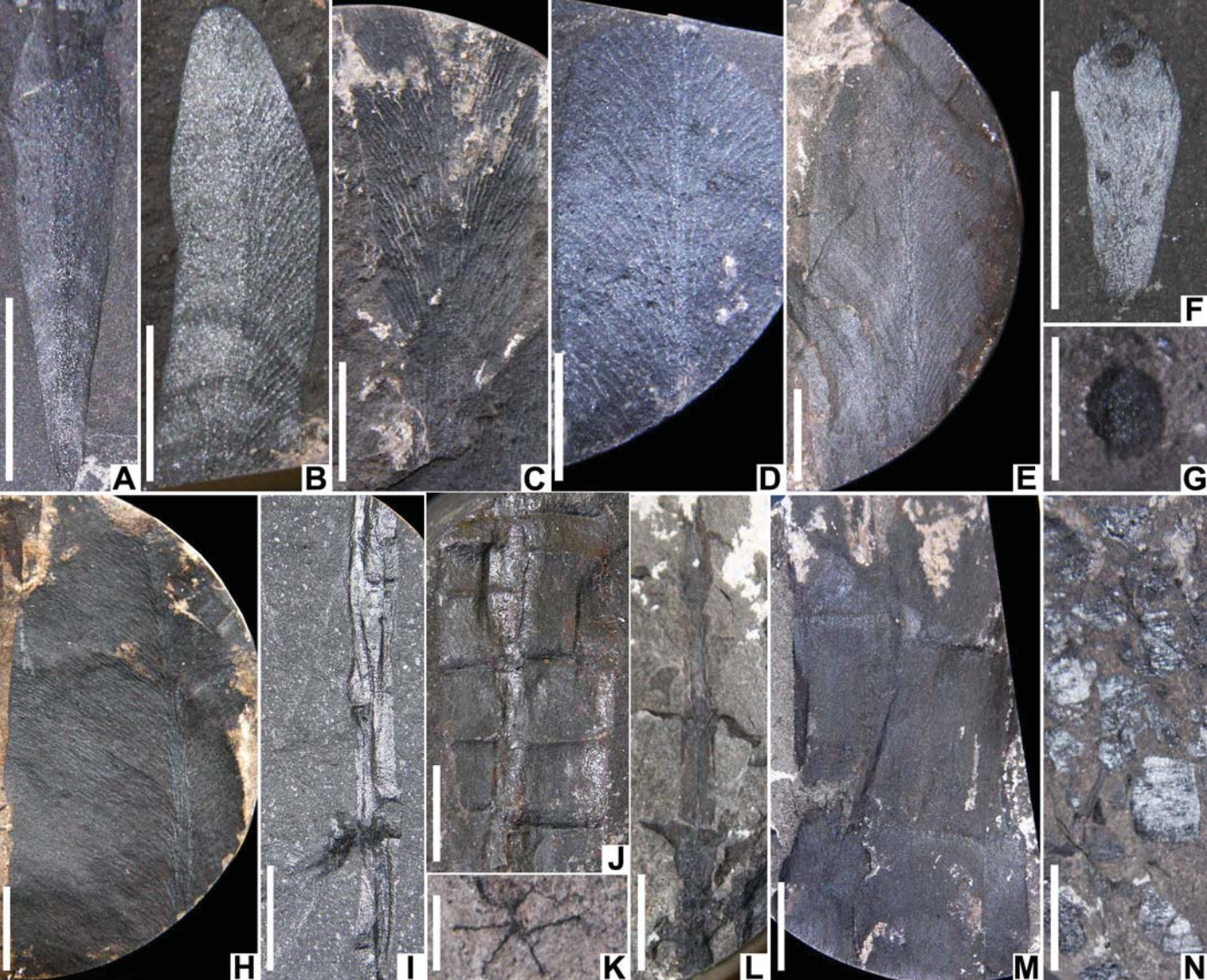
A
B
C
D
E
F
G
H
I
J
K
L
M
N

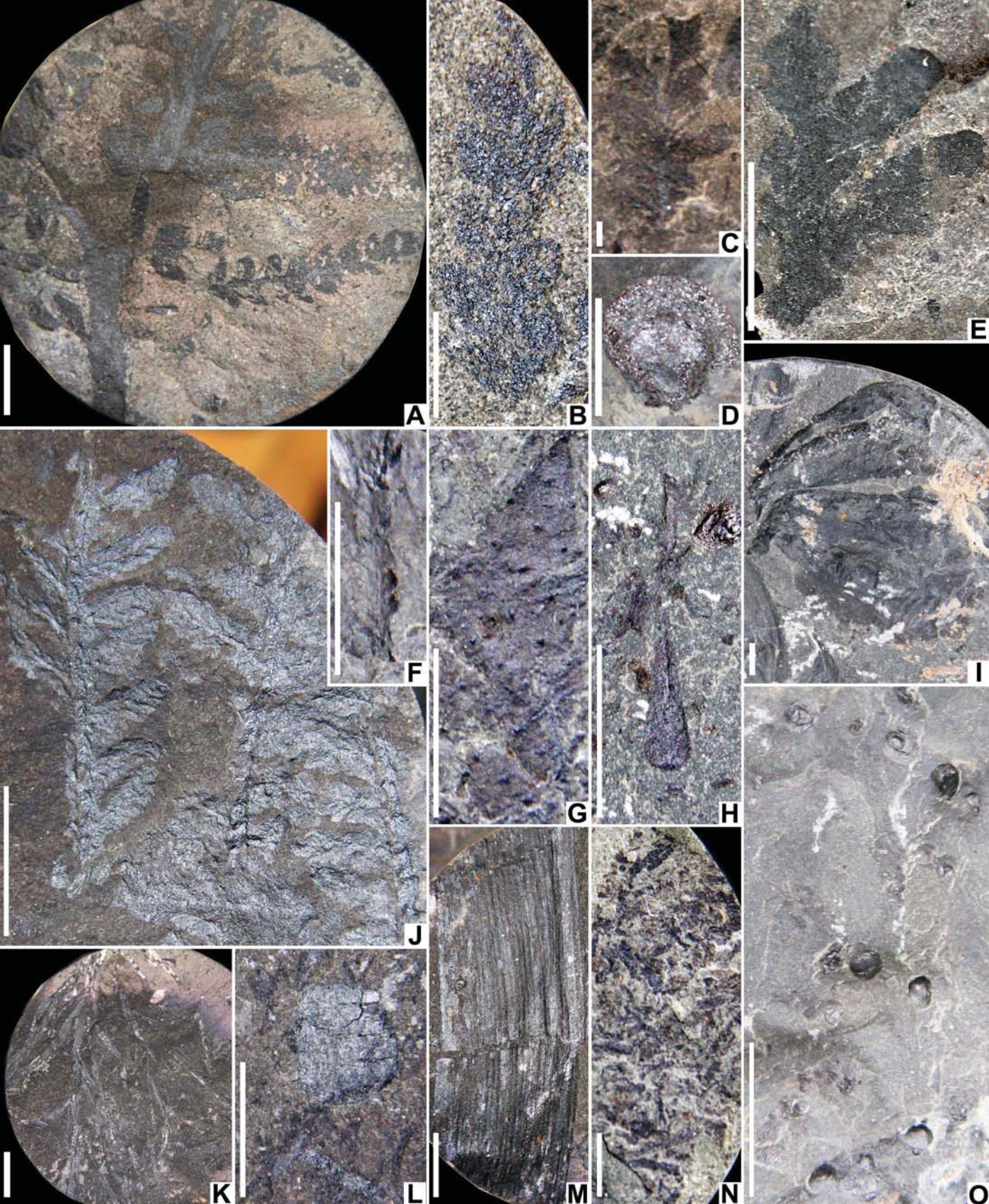
A
B
C
D
E
F
G
H
I
J
K
L
M
N
O

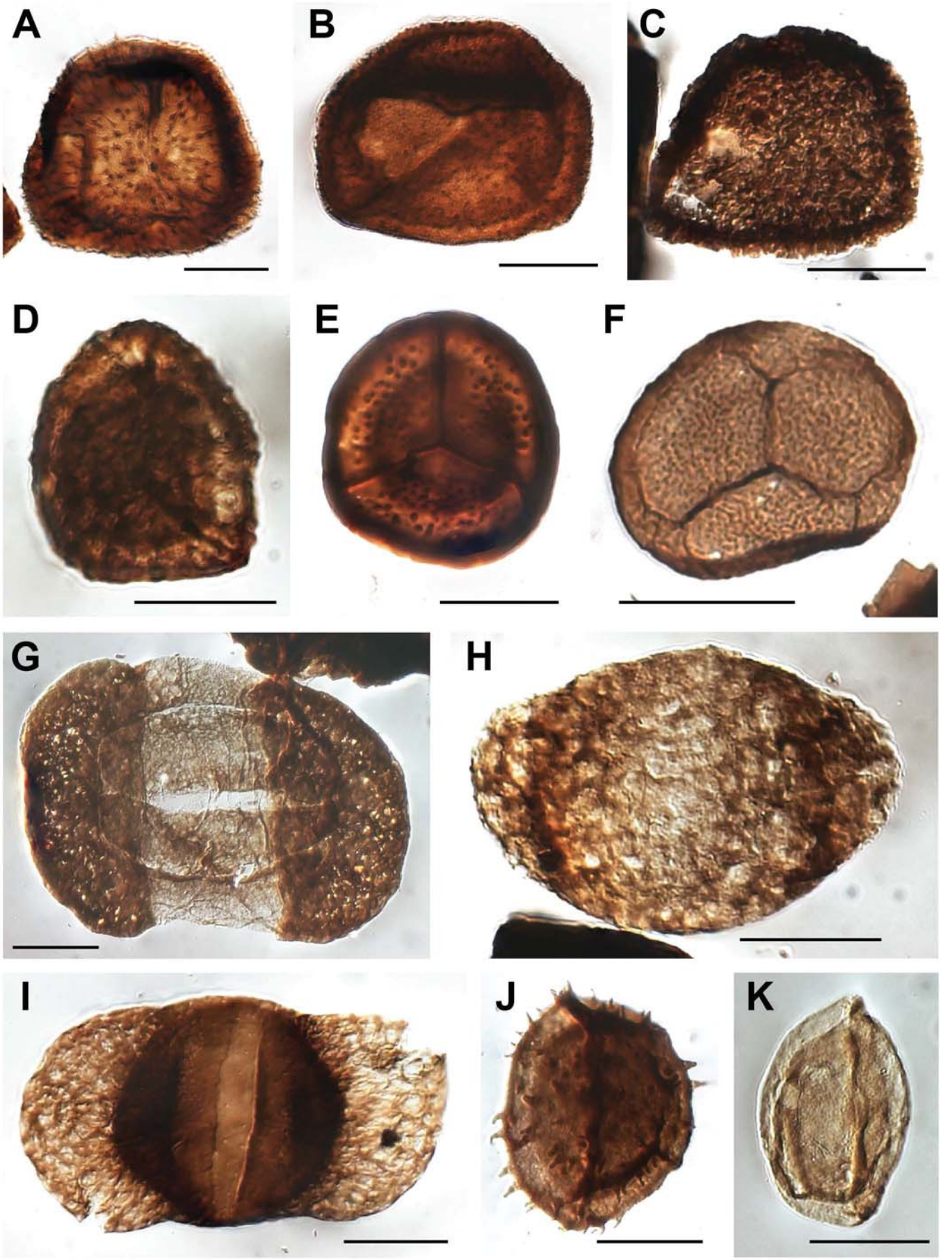
A
B
C
D
E
F
G
H
I
J
K

Global chronostratigraphy

Eastern Australia palynostratigraphy

Event timeline

Palynofloral

Macro floral

Sed.

Geo chem.

Terrestrial ecosystem stages

248

249

250

251

252

253

254

255

Ma

Triassic

Early Triassic

Olenekian

Spathian

Smithian

Ind.

G.

D.

Changhsingian

Wuch.

Permian

Lopingian

APT2

APT1

APP6

APP5

Aratrisporites tenuispinosus

Protohaploxypinus samoilovichii

Lunatisporites pellucidus

P. microcorpus

P. crenulata

'Dead zone'

Dulhuntyispora parvithola

Coarse baculate trilete spores

Lundbladispora springsurensis

Rewanispora foveolata

Lundbladispora sp. A

Limatulasporites spp.

Lunatisporites pellucidus

Aratrisporites spp.

Other pleuromeian spores (zonate trilete)

Dicroidium

Lepidopteris

Dulhuntyispora parvithola

Brevitriletes bulliensis

Triplexisporites playfordii

Thymospora spp.

Quadrisporites horridus

Leiosphere acritarchs

Playfordiaspora crenulata

Triquitrites proratus

Glossopteris

Vertebraria

Voltziales

'Red beds'

Organic-rich siltstone

Coal

CIA

Ni

CIA

Rising $\delta^{13}C_{org}$

Fluctuating $\delta^{13}C_{org}$

High $\delta^{13}C_{org}$

Ecosystem instability

Steady recovery

Suppressed recovery

Ecosystem collapse

?Destabilization

Stable glossopterid forests

EPE

Present study + Fielding et al. 2019 (Sydney Basin)

Legend

LAD

E Australia

this study

Abundances

regional

local

FAD

this study

E Australia

Meishan, S China (global stratotype section)
marine, ~15°N

Age (Ma) | Chronostrat. | m | Bed no. | $\delta^{13}C_{carb}$ (‰, VPDB) | $\delta^{13}C_{org}$ (‰, VPDB)

Triassic — Lower — Induan

Permian — Lopingian — Changhsingian

251.49 ± 0.064[1]

251.583 ± 0.086[1]

251.880 ± 0.031[1]

251.902 ± 0.024[1]

251.941 ± 0.037[1]

252.104 ± 0.089[1]

252.3 ± 0.3[2]

Bed 41 — 40 — 39 — 38 — 37 — 36 — 35 — 34 — 30–33 — 28–29 — 27a–b — 27c–d — 25–26 — 24a–e — 23 — 22 — 21 — 20 — 17–19 — 16

Ni peak

Marine extinction interval

-4 -2 0 2 4

-33 -31 -29 -27 -25

Initiation of gradual $\delta^{13}C_{org}$ decline

Chahe, S China
terrestrial, ~10°N

$\delta^{13}C_{org}$ (‰, VPDB)

m: -36 -32 -28 -24 -20

112 — 108 — 104 — 100 — 96 — 92 — 88 — 84 — 80 — 76 — 72 — 68 — 64

"Damaged zone" (Bourquin et al., 2018)

~PTB (Zhang et al., 2016)

FAD *Annalepis-Lepidopteris-Peltaspermum* flora

Coal LAD

Gigantopteris flora

Coal-forming plants

252.3 ± 0.07[3]

Age (Ma)

Bunnerong-1, Sydney Basin
terrestrial, ~65°S

m: 755 — 760 — 765 — 770 — 775 — 780 — 785 — 790 — 795 — 800 — 805 — 810 — 815 — 820

Lunatisporites pellucidus Zone

Protohaploxypinus microcorpus Zone

FAD *Lepidopteris*

Playfordiaspora crenulata Zone

Dulhuntyispora parvithola Zone

Ni peak

252.31 ± 0.07[5]

252.6 ± 0.04[4]

Coal-forming plants

Coal LAD

?

Glossopteris

Vertebraria

Terrestrial extinction interval

-30 -26 -22

Palynostrat. $\delta^{13}C_{org}$ (‰, VPDB)

Denison NS-20, Bowen Basin
terrestrial, ~55°S

m: 440 — 445 — 450 — 455 — 460 — 465

Lunatisporites pellucidus Zone

Protohaploxypinus microcorpus Zone

Playfordiaspora crenulata Zone

Dulhuntyispora parvithola Zone

Coal-forming plants

Coal LAD

-31 -27 -23

Palynostrat. $\delta^{13}C_{org}$ (‰, VPDB)

PTB

EPE